GEOMORPHOLOGICAL MAP OF NORTHERN XANTHE TERRA: A REFERENCE SITE FOR THE EXOMARS2022 ROVER LANDING SITE. T. Frueh[1,2], E. Hauber[2], S. Adeli[2], D. Tirsch[2], A. Nass[2], H. Hiesinger[1], and L. Pauw[1], [1]Institut für Planetologie, Westfälische Wilhelms-Universität Münster, Wilhelm-Klemm-Str.10, 48149 Münster, Germany, (thomas.frueh@uni-muenster.de), [2]Institute of Planetary Research, German Aerospace Center (DLR), Rutherfordstr. 2, 12489 Berlin, Germany.

Introduction: ESA's ExoMars rover will land in the Oxia Planum (OP) region [1,2], which was chosen for its ancient age, evidence for the sustained presence of water, the presence of layered deposits, and the potential for biosignature preservation [2]. While some of the geological characteristics have been studied in detail [3-5], other aspects are less well understood. In particular, it is unclear if the situation in OP is a unique one, or if the geologic setting is representative for Mars on a regional, or even a global scale. Specifically, the stratigraphic relationship of the geologic units in OP to the nearby ancient impact basin, Chryse Planitia, requires further study.

To test the hypothesis that OP is representative for a circum-Chryse geologic setting, we selected a site in northern Xanthe Terra (XT) (~9-13.5°N/315-318.5°E) to investigate key geologic features and compare them to OP. This site displays several characteristics similar to OP, making it a suitable reference site: The presence of phyllosilicates [6], the proximity to fluvial features [7-9], and the abundance of remnant buttes that might be indicative of widespread erosional processes [10]. Here we present preliminary results of our mapping and geologic analysis.

Data and Study Area: We used CTX, HRSC, HiRISE, and THEMIS image data for morphological mapping. Additional topographic information was derived from HRSC and MOLA DTMs. All datasets were integrated into a GIS environment. For uniformity with other studies [e.g., 11], the mapping was performed at a scale of 1:100,000.

The study area is approximately 225 × 190 km in size. The general elevation increases in height from north to south from approximately -2,960 m to -1,800 m. The lowland-highland boundary is expressed as a gradual slope, rather than a sharp topographic step in this region, similar to the situation in Oxia Planum. In the northern study area, the oldest and largest craters (> 10 km) are completely infilled. The extent of infilling decreases from the Chryse-basin towards south.

Units: In this section, the currently assigned units will be shortly explained, sorted by their relative age from old to young. It should be noted that these are working names of the units and not necessarily final. The current version of the map can be seen in Figure 1.

Cratered Plains. The unit is present in the southern part and is, relative to the other units, highly cratered. It also contains several large partly infilled ancient craters and parts of their strongly modified ejecta. Several small channels are present.

Phyllosilicate-Bearing Units. Two units in our study area, i.e., the light and dark plains, show a spectral signature of hydrous minerals [4]. The light plains lie on top of the dark plains. Where the light plains are eroded, the dark plains are visible. The presence of periodic bedrock ridges and ripples hint to intensive aeolian erosion [12]. Within the two units infilled and inverted channels are present. Both units show a polygonization at HiRISE scale. The polygonization of the light plains unit appears random, while the polygonization of the dark plains unit, at least where a HiRISE image is present, is NW orientated. The light plain unit is layered.

Ridged Plains. The ridged plains are superimposed on all previously mentioned units. They make up most of the surface of the study area and comprise numerous wrinkle ridges. The material also seems to be present in the infilled craters. The origin of this unit is still unclear, but a volcanic origin is likely.

Remnant Mounds. The two types of mapped mounds are buttes/knobs and mesas. Mesas are usually larger in diameter than buttes/knobs and have a flat top. Mesas can be tilted, and their height varies. Buttes/knobs have a rounded morphology. The exact stratigraphic relationship to the other units is still in progress. However, there are some hints to multiple mound formation phases, i.e., the different morphologies, the varying heights, complex relations with the Hypanis fan deposits, and the apparent overlap of mesas by buttes. Mesas, therefore, could be older than buttes/knobs. There is at least one layer of the flat plains that embays (and partly covers) the remnant mounds.

Fan Deposits. There are two fan deposits mapped. A smaller fan at an infilled crater at the end of a small channel within in the phyllosilicate-bearing units and two arms of the Hypanis fan deposits in the northwestern study area. Previous studies interpreted the fan to be of deltaic origin [8,9]. A dark unit is present as small patches close to the Hypanis deposits. This dark material is coarser and darker than the fan deposits and it does not show any layering in contrast to the fan deposits. The darker material partly covers the Hypanis fan. The close resemblance to the flat plains could make it difficult to spot this material further away from the Hypanis fan.

Shalbatana Vallis. The fluvially eroded valley is an outflow channel in the eastern study area. It cuts through all the previous mentioned units, besides the fan deposits. It also strongly eroded the flat plains into several blocks.

Collapsed Terrain. In the eastern part of the study area several collapse structures are present. Parts of Shalbatana Vallis show evidence for collapse. Some smaller collapsed terrains and single collapse holes are present mostly east of Shalbatana Vallis.

Conclusion: Northern Xanthe Terra displays various geological units, indicative of a history of extensive sedimentary and erosional processes in which the presence of water plays an important role.

References: [1] Vago, J. L. et al. (2015) *Sol. Syst. Res., 49,* 538–542. [2] Bridges, J. C. et al. (2018), *LPS XLIX,* #2177. [3] Vago, J. L. et al. (2017) *Astrobiol., 17,* 471–510. [4] Carter, J. et al., (2013) *J. Geophys. Res., 118*, 831–858. [5] Quantin-Nataf, C. et al. (2021) *Astrobiol., 21,* 994-1013. [6] Carter, J. et al. (2019) *Ninth Int. Conf. Mars,* #6175. [7] Hauber, E. et al. (2009) *Planet. Space Sci., 57,* 944–957. [8] Fawdon et al. (2018) *EPSL, 500*, 225–241. [9] Adler, J. B. et al. (2019) *Icarus, 319*, 885–908. [10] McNeil, J. et al. (2021) *J. Geophys. Res Planets, 126*. [11] Hauber, E. et al. (2021) *LPSC, 52*, #1947. [12] Silvestro, S. et al. (2021), *GRL, 48*, e91651.

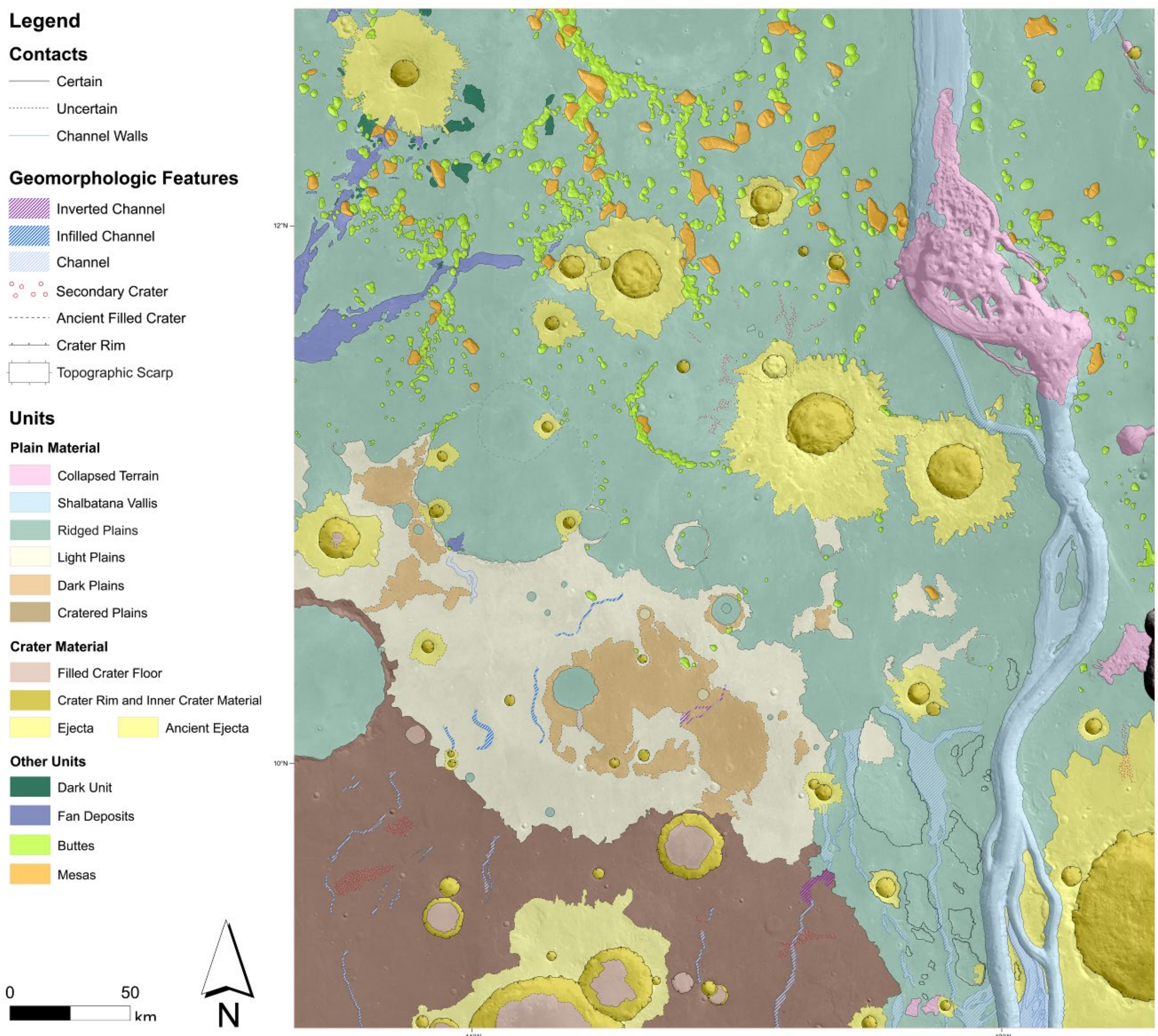

Figure 1. *Preliminary map of the study area projected on a HRSC image. Certain geological contacts are presented as solid lines and uncertain contacts as dashed lines. Uncertainty can be due to an early stage in the mapping progress, image quality, or due to the occurring geology.*